



■ KNEE

Comparison of tibial alignment parameters based on clinically relevant anatomical landmarks

A DEEP LEARNING RADIOLOGICAL ANALYSIS

**S. J. Jang,
K. N. Kunze,
Z. R. Brilliant,
M. Henson,
D. J. Mayman,
S. A. Jerabek,
J. M. Vigdorichik,
P. K. Sculco**

*From Hospital for
Special Surgery, New
York, New York, USA*

Aims

Accurate identification of the ankle joint centre is critical for estimating tibial coronal alignment in total knee arthroplasty (TKA). The purpose of the current study was to leverage artificial intelligence (AI) to determine the accuracy and effect of using different radiological anatomical landmarks to quantify mechanical alignment in relation to a traditionally defined radiological ankle centre.

Methods

Patients with full-limb radiographs from the Osteoarthritis Initiative were included. A sub-cohort of 250 radiographs were annotated for landmarks relevant to knee alignment and used to train a deep learning (U-Net) workflow for angle calculation on the entire database. The radiological ankle centre was defined as the midpoint of the superior talus edge/tibial plafond. Knee alignment (hip-knee-ankle angle) was compared against 1) midpoint of the most prominent malleoli points, 2) midpoint of the soft-tissue overlying malleoli, and 3) midpoint of the soft-tissue sulcus above the malleoli.

Results

A total of 932 bilateral full-limb radiographs (1,864 knees) were measured at a rate of 20.63 seconds/image. The knee alignment using the radiological ankle centre was accurate against ground truth radiologist measurements (inter-class correlation coefficient (ICC) = 0.99 (0.98 to 0.99)). Compared to the radiological ankle centre, the mean midpoint of the malleoli was 2.3 mm (SD 1.3) lateral and 5.2 mm (SD 2.4) distal, shifting alignment by 0.34° (SD 2.4°) valgus, whereas the midpoint of the soft-tissue sulcus was 4.69 mm (SD 3.55) lateral and 32.4 mm (SD 12.4) proximal, shifting alignment by 0.65° (SD 0.55°) valgus. On the intermalleolar line, measuring a point at 46% (SD 2%) of the intermalleolar width from the medial malleoli (2.38 mm medial adjustment from midpoint) resulted in knee alignment identical to using the radiological ankle centre.

Conclusion

The current study leveraged AI to create a consistent and objective model that can estimate patient-specific adjustments necessary for optimal landmark usage in extramedullary and computer-guided navigation for tibial coronal alignment to match radiological planning.

Cite this article: *Bone Jt Open* 2022;3-10:767–776.

Keywords: Knee alignment, Artificial intelligence, Machine learning, Mechanical alignment, Tibial alignment

Correspondence should be sent to Seong Jun Jang; email: sej4001@med.cornell.edu

doi: 10.1302/2633-1462.310.BJO-2022-0082.R1

Bone Jt Open 2022;3-10:767–776.

Introduction

Resection of the proximal tibia during total knee arthroplasty (TKA) is typically performed with a saw cut oriented perpendicular to the

mechanical axis in the coronal plane in order to obtain a desired tibial alignment.¹ For a traditional mechanical alignment target, the tibial cut is neutral to the tibial mechanical

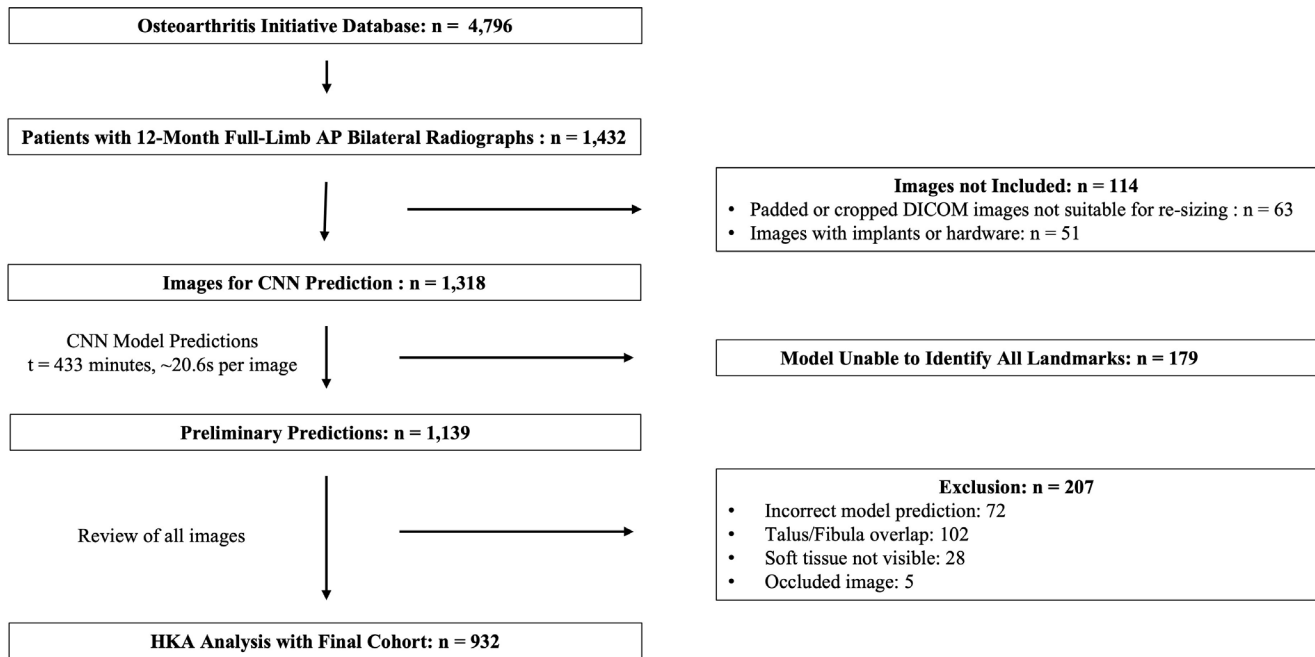


Fig. 1

Workflow for final application of knee alignment deep learning model on Osteoarthritis Initiative database.

axis to optimize contact forces and TKA longevity.²⁻⁵ Prior reports have shown that varus tibial alignment can result up to a 3.2 times greater risk of failure compared with neutral alignment and may even lead to collapse of the medial tibial bone.³ This misalignment may be accentuated and unavoidable in cases where the tibial mechanical and anatomical axes differ, such as in patients with proximal tibia bowing deformities.⁶ As such, identifying the ankle centre is imperative to obtain accurate tibial alignment measurements and potentially avoid adverse events associated with tibial component malposition in the coronal plane.

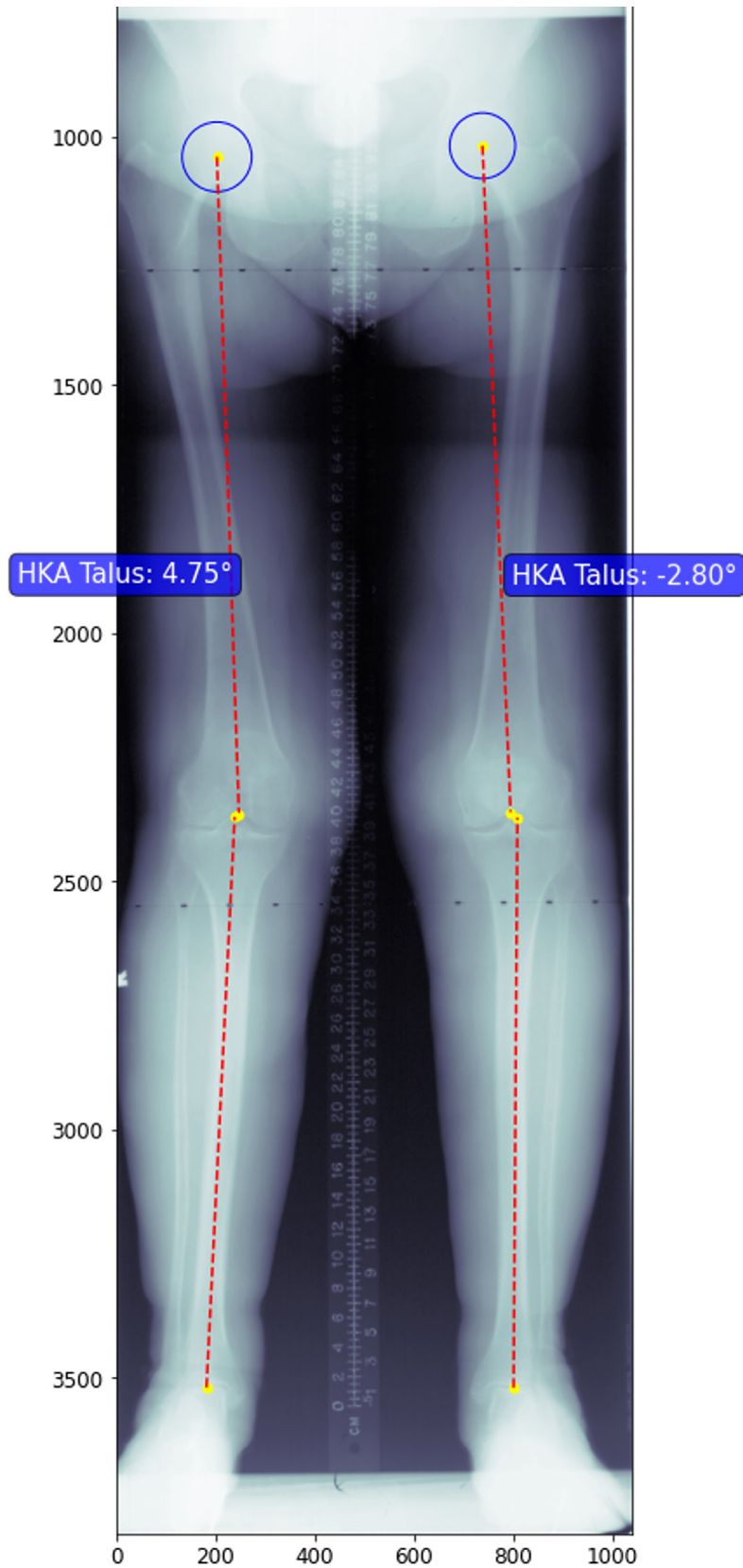
Contemporary methods of determining the optimal tibial resection alignment and rotation are performed predominately using three techniques: 1) with an extramedullary guide and drop rod using a combination or subset of anatomical landmarks, including the anterior tibial cortex or second metatarsal as a distal localization point, with the goal of defining the mechanical axis distal point as the ankle centre;^{1,7-9} 2) an intramedullary tibial alignment guide;^{5,10-12} or 3) robotic or computer-assisted navigation, using registration and calibration of anatomical landmarks (such as the medial and lateral malleoli) to confirm in real-time the desired orientation of tibial cut in the sagittal and coronal planes.¹³ However, radiologically, the tibial mechanical axis uses the tibial plafond centre or talus as the most distal extent; thus, contemporary methods of tibial mechanical alignment and desired resection planes in TKA may be subject to variations in the coronal and sagittal planes.⁵ This is especially relevant with extramedullary guides where the ankle centre

may be challenging to localize and is influenced by rotational differences between the proximal tibia and ankle.¹⁴ Though several attempts have been made to understand the associations between tibial alignment methods, landmarks including ankle centre of rotation, and resultant coronal plane resection angles, these studies are limited by small sample sizes and methodology subject to human error.^{6,7,13}

The use of artificial intelligence and deep learning to identify and compare clinically relevant anatomical landmarks for tibial bone resection is poised to overcome the limitations in subjective variability and measurement time burden inherent to human measurement. The purpose of the current study was to determine the accuracy and effect of using different radiological distal tibial anatomical landmarks for knee alignment in relation to a traditionally defined radiological ankle centre. The authors hypothesized that using anatomical landmarks that deviated further from the ankle centre, such as with the use of extramedullary guides dependent on soft-tissue, would lead to greater deviations from the radiological tibial mechanical alignment.

Methods

Patient and image selection. Patients with full limb standing radiographs from the Osteoarthritis Initiative (OAI) were included. The public database consists of data collected between 2004 and 2015 from 4,796 patients aged between 45 and 79 years. Institutional Review Board (IRB) approval was obtained at each institution involved in the creation of the database. Inclusion criteria were

**Fig. 2**

Hip-knee-ankle (HKA) angle, defined as angle subtended by the femoral and tibial mechanical axes (red lines). Positive values recorded as valgus and negative values recorded as varus.

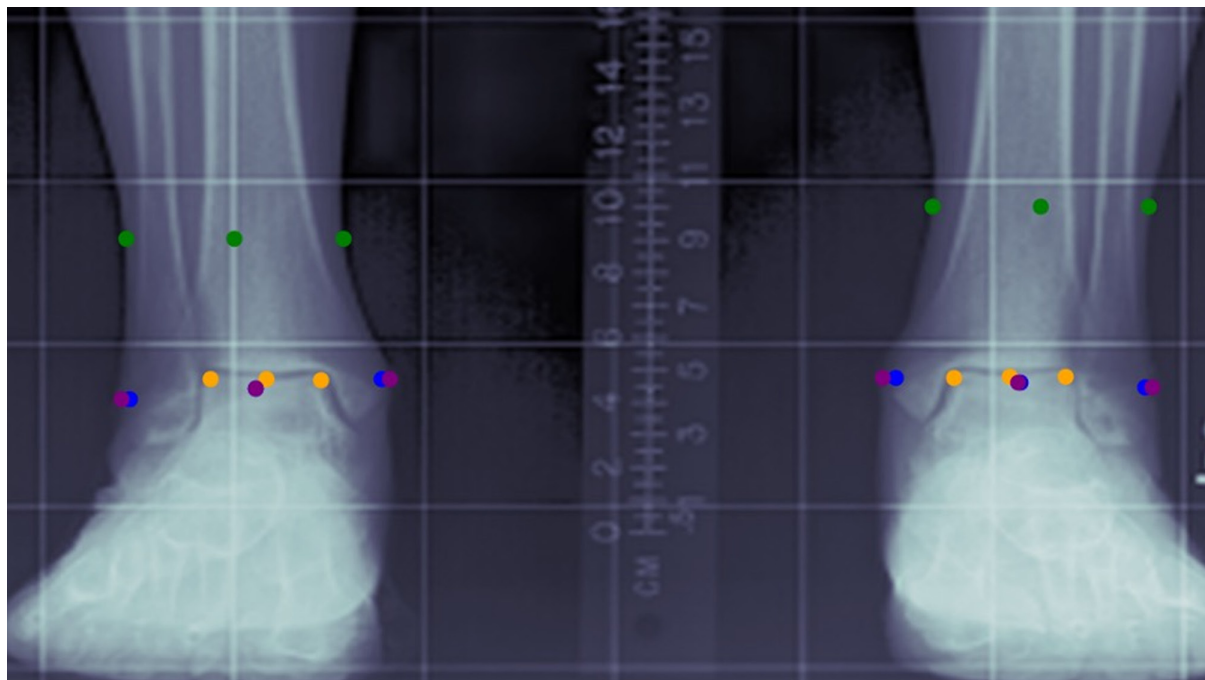


Fig. 3

Distal anatomical landmarks based on colour. Orange = radiological ankle center. Blue = medial and lateral malleoli. Purple = soft tissue overlying malleoli. Green = soft tissue sulcus.

individuals who had a full-limb radiograph available at the earliest timepoint (12 months from baseline enrolment). Exclusion criteria were patients who had already undergone a total or unicompartmental knee arthroplasty at the time of obtaining full limb radiographs (Figure 1).

Knee alignment and distal tibial alignment landmarks. The hip-knee-ankle (HKA) angle was measured as the angle subtended by the tibial and femoral mechanical axes. The femoral mechanical axis was defined as the line from the femoral head centre to the most central and superior point of the intercondylar notch of the distal femur. The tibial mechanical axis was defined as the line from the centre point between the most superior points on the two proximal tibial spines to a defined point on the distal talus/tibia. Negative angles were defined as varus and positive values as valgus (Figure 2).

We investigated four different distal anatomical landmarks to define the tibial mechanical axis that were clinically relevant to the use of extramedullary tibial guides and navigation-assisted knee surgery (Figure 3): 1) midpoint of the superior talus edge/tibial plafond (i.e. the radiological ankle centre);¹⁵ 2) midpoint of the line connecting the most prominent point on the medial malleoli and lateral fibula (i.e. intermalleolar line);¹³ 3) midpoint of the line connecting the soft-tissue directly overlying the malleoli; and 4) midpoint of the smallest soft-tissue width above the malleoli (i.e. ankle soft-tissue sulcus).

Convolutional neural networks. Convolutional neural networks (CNNs) are a type of deep learning network

used in computer vision tasks to identify features of interest in images. A U-Net is a specific type of CNN capable of classifying pixels as belonging to various objects.¹⁶ We trained U-Nets to identify bone and soft-tissue landmarks as objects on the radiographs to calculate knee alignment angles (Supplementary Material). The landmarks included the femoral head, femoral condyles, proximal tibial spines, talus, tibia, fibula, and soft-tissue (Figure 4). All training and validation data were manually annotated to establish ground truths for the model. Two separate models were created for bone and soft-tissue, and predictions were overlaid to conduct analyses regarding soft-tissue thickness (Figure 4).

Statistical analysis. The U-Net model's performance for landmark prediction was assessed using the multiclass dice coefficient and foreground accuracy.^{17,18} To ensure accurate HKA angle calculation against human measurements, the inter-class coefficient (two-way mixed, single score, ICC3) was calculated against available radiologist measurements from the OAI. For final analysis, the radiological ankle centre was used as the comparison control for other distal tibial landmarks. Every image was reviewed and calibrated by the vertical ruler. Paired *t*-tests were conducted to compare the approaches given that all four measurements were performed on each knee. Pearson's *R* correlation analyses were performed to determine the relationships between results and age, BMI, tibia length, and femur length. Furthermore, secondary analysis was conducted to determine what adjustment

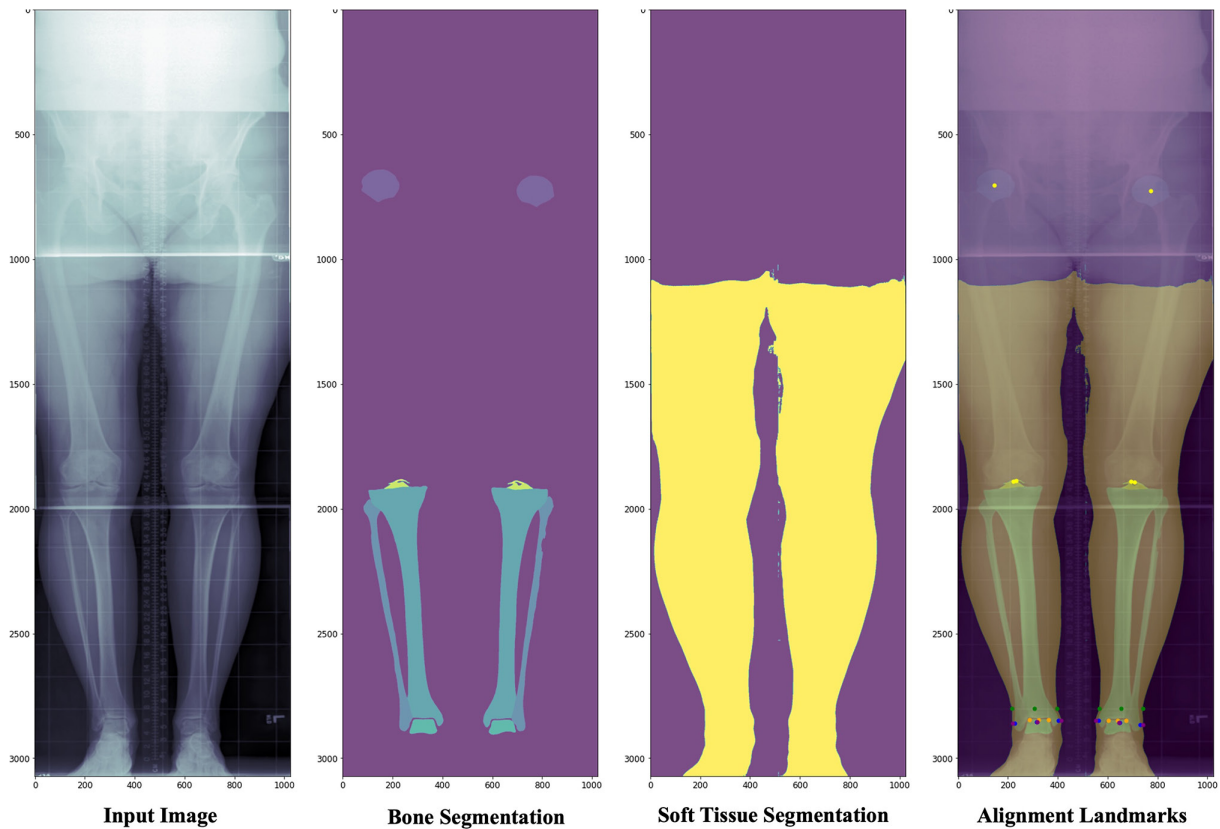


Fig. 4

Machine-learning workflow from input image to predicted alignment landmarks.

Table I. Hip-knee-ankle angle and comparison against Osteoarthritis Initiative radiologist measurements.

Landmark	Mean HKA angle (SD)	Mean paired difference from OAI measurements (SD)	Absolute paired difference > 2°	ICC against OAI measurements
Talus	-1.04 (3.67)	0.28 (0.69)	2.7%	0.99 (0.98 to 0.99)
Tibia/fibula malleoli	-0.69 (3.61)	0.63 (0.70)	4.8%	0.99 (0.98 to 0.99)
Soft-tissue over malleoli	-0.67 (3.62)	0.64 (0.70)	5.0%	0.99 (0.98 to 0.99)
Soft-tissue sulcus	-0.39 (3.58)	0.93 (0.82)	14.1%	0.98 (0.97 to 0.98)

HKA, hip-knee-ankle; ICC, inter-class correlation coefficient; OAI, Osteoarthritis Initiative.

ratio using the intermalleolar line would provide the HKA angle measured by the radiological ankle centre. All statistical analyses were conducted on a Jupyter Notebook (Python) using the Scipy.stats package and Statsmodel package.¹⁹

Results

Image cohorts. After image review and exclusion, knee alignment analysis was conducted on a final cohort of 932 patients (1,864 knees). The cohort's mean age was 61.5 years old (standard deviation (SD) 9.2), 53% (n = 491) were female, and mean BMI was 29.5 kg/m² (SD 4.5).

Deep learning workflow performance. Alignment angles (1,864 knees; 7,456 HKA angles) using the four different

distal tibial landmarks were calculated at a rate of approximately 20.63 seconds/image (328 total minutes). The bony landmark model had a dice coefficient of 0.87 and foreground accuracy of 0.94, whereas the soft-tissue model had a dice coefficient of 0.98 and foreground accuracy of 0.96 (Figure 4, model metrics in Supplementary Figures a and b). To ensure that the HKA angle was accurately measured by the machine-learning algorithm, the HKA using the radiological ankle centre was compared against available radiologist measurements from the OAI, resulting in strong interobserver reliability (ICC 0.99 (0.98 to 0.99))²⁰ (Table I).

HKA angle comparison by tibial landmarks. The mean HKA angle was -1.04° (SD 3.67°) using the radiological ankle centre (Table I). Compared against the radiological

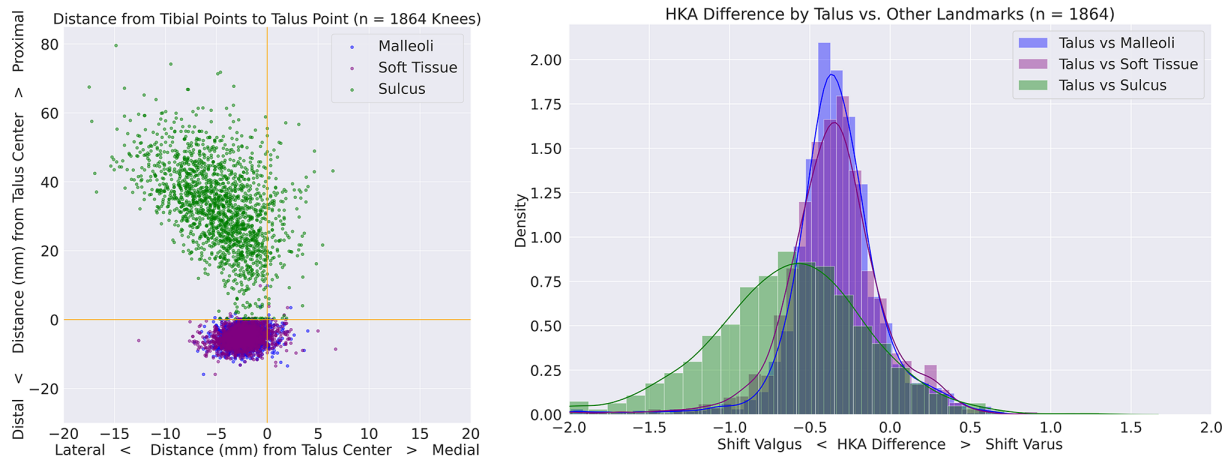


Fig. 5

Ankle centre offset (left, scatterplot) and hip-knee-ankle angle differences (right, histogram) based on landmarks relative to using the radiological ankle centre for cohort.

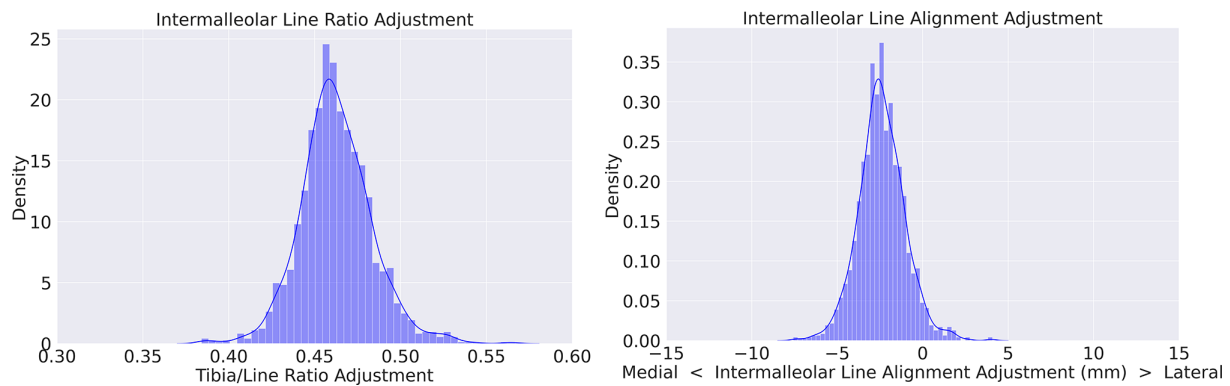


Fig. 6

Histograms of intermalleolar line ratio adjustment necessary for radiological ankle centre hip-knee-ankle angle replication. Left = ratio adjustment from medial malleoli. Right = mm adjustment from intermalleolar centre.

ankle centre, the midpoint of the intermalleolar line was 2.27 mm (SD 1.29) lateral and 5.17 mm (SD 2.44) distal. The HKA angle was significantly different (mean -0.69° (SD 3.61°), $p = 0.005$) and 0.34° (SD 0.32°) more valgus (paired differences against radiological ankle centre). The midpoint of the soft-tissue overlying the malleoli was 2.39 mm (SD 1.58) lateral and 5.17 mm (SD 2.44) distal to the radiological ankle centre. The HKA angle was significantly different (mean -0.67° (SD 3.62°), $p = 0.003$) and 0.37° (SD 0.35°) more valgus using this landmark. Finally, the midpoint of the soft-tissue sulcus above the malleoli (sulcus) was 4.69 mm (SD 3.55) lateral and 32.40 mm (SD 12.45) proximal to the radiological ankle centre. The HKA angle was significantly different (mean -0.39° (SD 3.58°), $p < 0.001$) and 0.65° (SD 0.55°) more valgus (Figure 5).

BMI had a weak correlation with soft-tissue overlying the tibia ($r = 0.30$, $p < 0.001$) and fibula ($r = 0.33$, $p < 0.001$); however, age, BMI, tibia length, and femur length had weak correlations with knee alignment differences

between the different landmarks from the radiological ankle centre ($r < 0.10$).

Proposed adjustment to approximate ankle joint centre during TKA. To determine the necessary tibial landmark adjustment using the intermalleolar line to replicate the HKA angle formed by the radiological ankle centre, ratios of the intermalleolar width from the medial malleoli were calculated for each knee. On the intermalleolar line, measuring a point at a mean 46.3% (SD 2.1%) of the intermalleolar width from the medial malleoli resulted in knee alignment measurements consistent with the radiological ankle centre. This adjustment translated to a 2.38 mm (SD 1.37) shift medially from the intermalleolar line centre to match the radiological ankle joint centre (Figure 6).

Discussion

This study's main findings are as follows: 1) a novel deep-learning algorithm was developed, capable of accurately

and rapidly calculating the HKA angle using four different tibial anatomical landmarks; 2) comparison among HKA measurement methods demonstrated that using the soft-tissue sulcus proximal to the malleoli (i.e. where the distal ankle clamp of an extramedullary guide usually attaches) results in the largest coronal plane deviation from the radiological ankle centre; 3) the algorithm was able to quantify a precise adjustment necessary to match a HKA measured using the radiological ankle joint centre, suggesting that a point a mean 46.3% of the intermalleolar width from the medial malleoli (or 2.38 mm varus adjustment) resulted in knee alignment measurements identical to the radiological ankle centre in this population.

The deep-learning model developed in this study measured 932 bilateral full-limb radiographs (1,864 knees) at a rate of approximately 20.63 seconds/image. The dice segmentation coefficient and foreground accuracy, which assessed the spatial overlap between the deep-learning model predictions and established ground truth annotations were above > 0.85 for both the bone and soft-tissue segmentation models. This indicates excellent segmentation results in accordance with previous studies investigating this approach for automated deep-learning orthopaedic measurements.^{21,22} However, compared to previous studies, we also use segmentation to outline soft-tissue in addition to bone on plain radiographs to calculate the HKA angle.

Furthermore, the knee alignment angles using the radiological ankle centre were highly accurate against ground truth measurements made by trained radiologists. This is an important finding, suggesting that the model predictions of tibial alignment are in accordance with radiological measurements made in clinical practice. Furthermore, the objectivity and speed of the algorithm may have several clinical benefits. Indeed, subjectivity inherent in human measurement may result in inter-measurer and inter-subject variations, especially when radiographs are difficult to measure because of rotation or quality. This presents challenges when alignment measurements are needed for research purposes or preoperative planning.²³ Hess et al²⁴ performed a systematic review of 15 studies in patients with osteoarthritic knees to better understand coronal alignment variability, ultimately concluding that significant variation exists in the HKA angle as well as femoral and tibial mechanical angles across populations, which may not be appropriately accounted for when planning TKA. Deep-learning-based identification of bony landmarks can produce objective measurements and overcome subjective limitations, allowing for more accurate assessments and less variation in preoperative planning. This has been demonstrated by multiple studies for HKA,^{25,26} although none have leveraged deep learning to explore HKA based on different landmarks other than

the radiological ankle centre. Here, we present the use of deep learning to measure the HKA based on several clinically relevant landmarks used intraoperatively for tibial alignment. Future studies are warranted to evaluate the performance of the deep-learning model in external populations to confirm accuracy and reliability across diverse cohorts of patients.

This study also provides insight into the quantitative differences among clinically relevant distal reference points and emphasizes the importance of understanding the magnitude of deviation from the true ankle centre. Compared to the radiological ankle centre, significant coronal plane variations were identified based on the distal tibial landmark. Specifically, the mean midpoint of the malleoli was 2.3 mm (SD 1.3) lateral and 5.2 mm (SD 2.4) distal to the ankle centre, and shifted knee alignment valgus by 0.34° (SD 2.4°). Using the soft-tissue sulcus, the midpoint of measurement shifted 4.69 mm (SD 3.55) lateral and 32.4 mm (SD 12.4) proximal to the ankle centre, and shifted knee alignment valgus by 0.65° (SD 0.55°). Although a difference of 0.28° to 0.93° between landmark use may represent small clinical significance, recent studies investigating the use of HKA angles in phenotyping knees undergoing TKA use HKA angle cutoffs of -2° to 2° .²⁷ Thus, these small deviations can lead to systematic differences in classification of knees in varus and valgus simply based on the landmarks used for measurements for both research and clinical application.

Furthermore, the statistically significant variations from the radiological ankle centre reported in this study are consistent with literature examining associations between anatomical variation and coronal plane alignment. Cinotti et al²⁸ reported that the trajectory of the anterior tibial cortex assumes three patterns including curved, straight, and mixed courses, which intersect the mechanical axis at different points. Depending on the course, the difference in the angle between the cortex and mechanical axis exceeded 3° in more than 35% of cases. Asada et al⁶ retrospectively examined 102 CT scans in patients with osteoarthritic knees and used both the tibial anteroposterior (AP) and transmalleolar (TMA) axis as rotational reference axes of the knee and ankle joint, respectively. They found that the mean offset distances with reference from the tibial AP and TMA axes were 1.8 mm and 3.0 mm medial from the intermalleolar midpoint, respectively. The proximal tibia cut varus deviations ranged from 0.1° to 0.7° excluding the skin, and 0.1° to 1.1° including the skin. Finally, Siston et al¹³ evaluated the accuracy of five anatomical and two kinematic methods of determining the ankle centre in 11 subjects using MRI. They found that establishing the midpoints of the most medial and lateral aspects of the malleoli was the most accurate method, conferring a mean 4.5 mm of lateral error. Similar relationships have been identified using computer-assisted navigation.⁷ Thus, this trend

towards lateral deviation of the assumed ankle centre is consistent with this study's results, and contributes plausibility to the ability of deep-learning methods to accurately quantify the true and projected tibial alignment. Regardless of the alignment target, whether kinematic or mechanical, a model to reliably identify the ankle centre would be beneficial in preoperative planning and surgical execution.

Based on this study, when performing tibial resections with extramedullary mechanical guides with the distal ankle clamp centred within the soft-tissue sulcus, a medial shift of 4.69 mm (approximately 5 mm) is recommended. Care should be taken to perform secondary checks with either the anterior tibial cortex, anterior tibial tendon, or second metatarsal due to the variability required for medial translation (± 3.55 mm). However, given that prior literature has suggested that the use of extramedullary guides may lead to a higher incidence of tibial tray malalignment due to mechanical axis outliers,⁵ and in conjunction with the current findings, we recommend the use of the intermalleolar line to approximate the ankle joint centre, as dependence on the soft-tissues with other methods may result in more significant valgus deviation.

Given the above findings, we also reported the necessary clinical adjustment in tibial alignment using the intermalleolar line to counteract the coronal deviations. Measuring a point at 46.3% (SD 2.1%) of the intermalleolar width from the medial malleoli resulted in knee alignment measurements consistent with the radiological ankle centre. This ratio provides valuable information from a large cohort of patients for computer navigation and robotic systems that use a predetermined ratio for determining the ankle centre based on medial and lateral malleoli intraoperative registration. This translated to a 2.38 mm medial, or varus, adjustment when assessing tibial alignment. Interestingly, we found that BMI did not influence the mechanical alignment differences or need for adjustments, which is consistent with previous literature.²⁹ Regardless, results from prior literature and this study suggests an overall tendency towards valgus misalignment that should be addressed to approximate the ankle centre during TKA. Though this proposed adjustment was specific to the current population, the inherent function of deep learning which uses patient-specific radiographs allows for the rapid calculations necessary for specific adjustments necessary on a patient-by-patient basis. Future studies investigating the use of these preoperative deep-learning patient-specific adjustment ratios, intraoperatively, are of interest to determine if they result in more accurate targeted knee alignment postoperatively in manual, computer-assisted, and robotic TKA.

First, the current study represents the performance of the development and internal validation of a deep-learning model, and external validation of this model is

imperative to confirm performance in patient populations that may differ from those included in the OAI. Though the proposed coronal plane adjustment to measure the true ankle centre was determined to be 46.3% or 2.38 mm in this specific population, this adjustment needs to be confirmed in independent populations and with extramedullary and/or computer navigation guides. Second, measurements of HKA angles using landmarks other than the tibial plafond centre were not directly compared against radiologist readings in a large cohort, as these measurements were not available in the OAI and are not routinely conducted on radiographs. Rather, the measurements of HKA angles using other landmarks such as soft-tissue and malleoli were compared against those of the HKA angle using the tibial plafond as a reference. All images were individually reviewed to ensure soft-tissue and malleoli landmarks were accurate to produce correct measurements before final analysis. As such, a proportion of images were excluded for final analysis after human review due to incorrect model prediction. However, we argue that the purpose of this study was to leverage deep learning to explore measurements rather than to create a fully robust deep-learning model capable of measuring every possible image accurately. Third, only AP hip-to-ankle standing radiographs were available in the OAI database, and therefore the influence of tibial landmark selection on sagittal parameters such as tibial slope and their association with coronal plane deviations could not be studied. These coronal plane deviations can be common in patients with osteoarthritis, and have implications for surgical planning, overall postoperative alignment, and implant survivorship.^{4,30,31} Thus, the relationship between coronal alignment and important metrics (clinical, functional, survivorship) in the context of measurements made by the deep-learning model remain uninvestigated and are of interest for future studies.

In summary, the current study leveraged AI to create a rapid and objective model that can estimate patient-specific adjustments necessary to target the radiological centre of the ankle. We found that the magnitude of medial translation depends on the selected anatomical landmarks which differ based on whether an extramedullary or computer-guided navigation technique is used. For mechanical alignment with extramedullary jigs, additional care must be taken to confirm accurate alignment as the larger variability in the required medial shift may contribute to tibial alignment error.



Take home message

- A deep-learning radiological analysis revealed deviations in tibial mechanical axis measurements using different anatomical landmarks relevant to total knee arthroplasty.
- A point at 46.2% of the distal limb intermalleolar line width from the medial malleoli results in knee alignment identical to the radiological talar/tibial plafond ankle centre.

Supplementary material



Methods on deep-learning model creation and performance.

References

- Chiu KY, Yau WP, Ng TP, Tang WM. The accuracy of extramedullary guides for tibial component placement in total knee arthroplasty. *Int Orthop*. 2008;32(4):467–471.
- Green GV, Berend KR, Berend ME, Glisson RR, Vail TP. The effects of varus tibial alignment on proximal tibial surface strain in total knee arthroplasty: The posteromedial hot spot. *J Arthroplasty*. 2002;17(8):1033–1039.
- Fang DM, Ritter MA, Davis KE. Coronal alignment in total knee arthroplasty: just how important is it? *J Arthroplasty*. 2009;24(6 Suppl):39–43.
- van Hamersveld KT, Marang-van de Mheen PJ, Nelissen R. The effect of coronal alignment on tibial component migration following total knee arthroplasty: A cohort study with long-term radiostereometric analysis results. *J Bone Joint Surg Am*. 2019;101-A(13):1203–1212.
- Patil S, D'Lima DD, Fait JM, Colwell CW. Improving tibial component coronal alignment during total knee arthroplasty with use of a tibial planing device. *J Bone Joint Surg Am*. 2007;89-A(2):381–387.
- Asada S, Mori S, Inoue S, Tsukamoto I, Akagi M. Location of the ankle center for total knee arthroplasty. *Knee*. 2017;24(1):121–127.
- Vejjaiviva A, Sriphiroom P, Saepoo C, Ounjitti W, Suwansaiphon S. Accuracy of ratio for centre of the ankle method as a landmark for proximal tibial cutting in computer assisted total knee arthroplasty compared with extramedullary method. *CAOS EPIC Series in Health Sciences*. 2019;3:388–391.
- Men J, Liang HG, Wang ZW, Sun P, Feng W. Efficacy analysis of selection of distal reference point for tibial coronal plane osteotomy during total knee arthroplasty: A literature review. *Orthop Surg*. 2021;13(5):1682–1693.
- Tsukeoka T, Lee TH, Tsuneizumi Y, Suzuki M. The tibial crest as a practical useful landmark in total knee arthroplasty. *Knee*. 2014;21(1):283–289.
- Cashman JP, Carty FL, Synnott K, Kenny PJ. Intramedullary versus extramedullary alignment of the tibial component in the Triathlon knee. *J Orthop Surg Res*. 2011;6:44.
- Talmo CT, Cooper AJ, Wuerz T, Lang JE, Bono JV. Tibial component alignment after total knee arthroplasty with intramedullary instrumentation: a prospective analysis. *J Arthroplasty*. 2010;25(8):1209–1215.
- Teter KE, Bregman D, Colwell CW. Accuracy of intramedullary versus extramedullary tibial alignment cutting systems in total knee arthroplasty. *Clin Orthop Relat Res*. 1995;321:106–110.
- Siston RA, Daub AC, Giori NJ, Goodman SB, Delp SL. Evaluation of methods that locate the center of the ankle for computer-assisted total knee arthroplasty. *Clin Orthop Relat Res*. 2005;439:129–135.
- Mizu-Uchi H, Kido H, Chikama T, Kamo K, Kido S, Nakashima Y. The adjustment of the rotational alignment of the distal end of the extramedullary guide to the anteroposterior axis of the proximal tibia in total knee arthroplasty. *J Knee Surg*. 2021.
- Iseki Y, Takahashi T, Takeda H, et al. Defining the load bearing axis of the lower extremity obtained from anterior-posterior digital radiographs of the whole limb in stance. *Osteoarthr Cartil*. 2009;17(5):586–591.
- Ronneberger O, Fischer P, Brox T (eds). *U-Net: Convolutional Networks for Biomedical Image Segmentation*. Springer International Publishing, 2015.
- Steyerberg EW, Vickers AJ, Cook NR, et al. Assessing the performance of prediction models: a framework for traditional and novel measures. *Epidemiology*. 2010;21(1):128–138.
- Zou KH, Warfield SK, Bharatha A, et al. Statistical validation of image segmentation quality based on a spatial overlap index. *Acad Radiol*. 2004;11(2):178–189.
- Virtanen P, Gommers R, Oliphant TE, et al. SciPy 1.0: fundamental algorithms for scientific computing in Python. *Nat Methods*. 2020;17(3):261–272.
- Koo TK, Li MY. A guideline of selecting and reporting intraclass correlation coefficients for reliability research. *J Chiropr Med*. 2016;15(2):155–163.
- Schwartz JT, Cho BH, Tang P, et al. Deep learning automates measurement of spinopelvic parameters on lateral lumbar radiographs. *Spine (Phila Pa 1976)*. 2021;46(12):E671–E678.
- Rouzrok P, Wyles CC, Philbrick KA, et al. A deep learning tool for automated radiographic measurement of acetabular component inclination and version after total hip arthroplasty. *J Arthroplasty*. 2021;36(7):2510–2517.
- Nam D, Vajapey S, Nunley RM, Barrack RL. The impact of imaging modality on the measurement of coronal plane alignment after total knee arthroplasty. *J Arthroplasty*. 2016;31(10):2314–2319.
- Hess S, Moser LB, Amsler F, Behrend H, Hirschmann MT. Highly variable coronal tibial and femoral alignment in osteoarthritic knees: a systematic review. *Knee Surg Sports Traumatol Arthrosc*. 2019;27(5):1368–1377.
- Schock J, Truhn D, Abrar DB, et al. Automated analysis of alignment in long-leg radiographs by using a fully automated support system based on artificial intelligence. *Radiol Artif Intell*. 2021;3(2):e200198.
- Tack A, Preim B, Zachow S. Fully automated assessment of knee alignment from full-leg X-rays employing a “YOLOv4 And Resnet Landmark regression Algorithm” (YARLA): data from the Osteoarthritis Initiative. *Comput Methods Programs Biomed*. 2021;205:106080.
- MacDessi SJ, Griffiths-Jones W, Harris IA, Bellemans J, Chen DB. Coronal Plane Alignment of the Knee (CPAK) classification. *Bone Joint J*. 2021;103-B(2):329–337.
- Cinotti G, Ripani FR, Sinno E, Sarti S, LaTorre G, Giannicola G. Revisiting the tibial crest as reference for the mechanical alignment of the tibial component in total knee arthroplasty: a cadaveric study on Caucasian tibiae. *Musculoskelet Surg*. 2021;105(2):161–166.
- Compton J, Owens J, Otero J, Noiseux N, Brown T. Extramedullary guide alignment is not affected by obesity in primary total knee arthroplasty. *J Knee Surg*. 2021;34(10):1076–1079.
- Stan G, Orban H, Gruionu L, Gheorghe P. Coronal malposition effects in total knee arthroplasty: a finite element analysis. *Eur J Orthop Surg Traumatol*. 2013;23(6):685–690.
- Vandekerckhove P-J, Teeter MG, Naudie DDR, Howard JL, MacDonald SJ, Lanting BA. The impact of coronal plane alignment on polyethylene wear and damage in total knee arthroplasty: A retrieval study. *J Arthroplasty*. 2017;32(6):2012–2016.

Author information:

- S. J. Jang, BA, Medical Student, Weill Cornell Medical College, New York, New York, USA; Department of Orthopedic Surgery, Hospital for Special Surgery, New York, New York, USA.
- K. N. Kunze, MD, Resident
- M. Henson, MS, Research Assistant
Department of Orthopedic Surgery, Hospital for Special Surgery, New York, New York, USA.
- Z. R. Brilliant, BS, Medical Student, Adult Reconstruction and Joint Replacement Service, Hospital for Special Surgery, New York, New York, USA; University of Maryland School of Medicine, Baltimore, Maryland, USA.
- D. J. Mayman, MD, Orthopaedic Surgeon
- S. A. Jerabek, MD, Orthopaedic Surgeon
- J. M. Vigdorichik, MD, Orthopaedic Surgeon
- P. K. Sculco, MD, Orthopaedic Surgeon
Department of Orthopedic Surgery, Hospital for Special Surgery, New York, New York, USA; Adult Reconstruction and Joint Replacement Service, Hospital for Special Surgery, New York, New York, USA.

Author contributions:

- S. J. Jang: Writing – original draft, Data curation, Formal analysis, Investigation, Methodology.
- K. N. Kunze: Writing – original draft, Data curation, Formal analysis, Investigation, Methodology.
- Z. R. Brilliant: Data curation, Investigation, Writing – review & editing.
- M. Henson: Writing – original draft, Data curation, Investigation, Project administration.
- D. J. Mayman: Conceptualization, Investigation, Formal analysis, Writing – review & editing.
- S. A. Jerabek: Conceptualization, Investigation, Writing – review & editing.
- J. M. Vigdorichik: Conceptualization, Investigation, Writing – review & editing.
- P. K. Sculco: Conceptualization, Investigation, Supervision, Writing – review & editing.

Funding statement:

- The authors received no financial or material support for the research, authorship, and/or publication of this article.

ICMJE COI statement:

- J. M. Vigdorichik reports grants from Corin USA, and consulting fees from DePuy, Intellijoint Surgical, Medacta, and Stryker, leadership or fiduciary role in the American Association of Hip and Knee Surgeons, the British Editorial Society of Bone & Joint Surgery, stock or stock options in Corin USA, Cuptimize, Intellijoint Surgical, and Motion Insights, all of which are unrelated to this study. P. K. Sculco reports grants from Intellijoint Surgical, consulting fees from DePuy, EOS Imaging, Intellijoint Surgical, Lima Corporate, and Zimmer, and payments or honoraria for lectures, presentations, speakers bureaus, manuscript writing or educational events from DePuy, EOS Imaging, and Intellijoint Surgical, and stock or stock options to Intellijoint Surgical and Parvizi Surgical Innovation, all of which are unrelated to this study. D. J. Mayman reports royalties from Orthalign and Smith & Nephew, and consulting fees from Stryker, and stock or stock options from Imagen, Orthalign, Smith & Nephew, Wishbone, MiCare Path, and Cymedica, all of which are unrelated

to this study. S. A. Jerabek reports royalties, consulting fees, payment or honoraria for lectures, presentations, speakers bureaus, manuscript writing or educational events, and support for attending meetings and/or travel from Stryker, and stock or stock options from Imagen, all of which are unrelated to this study. Each author certifies that he or she has no commercial associations (e.g., consultancies, stock ownership, equity interest, patent/licensing arrangements, etc.) that might pose a conflict of interest in connection with the submitted article.

Ethical review statement:

- This study was conducted using a public de-identified online database (Osteoarthritis Initiative) for secondary data analysis. The creation of the database was approved by the institutional review board at the respective institutions involved in the OAI.

Open access funding

- The authors confirm that the open access fee for this study was self-funded.

© 2022 Author(s) et al. This is an open-access article distributed under the terms of the Creative Commons Attribution Non-Commercial No Derivatives (CC BY-NC-ND 4.0) licence, which permits the copying and redistribution of the work only, and provided the original author and source are credited. See <https://creativecommons.org/licenses/by-nc-nd/4.0/>